Absolute dual-polarization radar calibration: temperature dependence and stability with focus on antenna-mounted receivers and noise source generated reference signal

Dennis Vollbracht[1], Maurizio Sartori [2], Marco Gabella[2],

[1]*Selex ES GmbH, Raiffeisenstrasse 10, 41470 Neuss, Germany*

[2,]*MeteoSvizzera, Via ai Monti 146, 6605 Locarno-Monti, Svizzera*

(Dated: 18 July 2014)

1 Introduction

In 2011 MeteoSwiss started renewing and extending its operational C-band weather radar network. The three existing radars have been replaced by state-of-the-art polarimetric Doppler radars with antenna-mounted receivers (AMR); two additional systems at high altitude are foreseen and one of them became recently (May 2014) operational. After having opted for polarimetric systems, MeteoSwiss had also considered whether to choose an innovative solution based on antenna-mounted digital receivers; remarkable advantages of such solution (with respect to the conventional one, which is receivers next to the transmitter (TX) in the technical room) are:

- Reduced receive path losses;
- Avoiding expensive dual-pol rotary joint, which also introduce differential errors in amplitude and phase
- Avoiding amplitude and phase differential errors caused by azimuth and elevation rotary joints (in the elegant antenna-mounted solution, in-fact, the magic-tee is obviously after the two rotary joints of the TX chain).

After two years of operational atmospheric monitoring, MeteoSwiss is satisfied with the AMR system concept choice, also in view of the necessary constrains related to maintenance and temperature control inside the radome.

Nevertheless, absolute radar calibration is indeed a challenging topic. Radar manufacturers typically provide stable continuous wave RF generators known as internal test signal generators (ITSG) as an absolute reference signal to calibrate the dBZ value for the computation of the weather radar equation with a known dBm value at the calibration reference point.

MeteoSwiss decided to use a noise source as absolute reference for calibrating their radar systems. Most important benefits of the realized calibration solution are the high temperature stability of the noise source, online monitoring of TR Limiter losses, online noise figure measurements, Hi-Low Calibration for the Dynrex [1] solution (dynamic range extension) and the online absolute calibration of the high sensitivity channel, since most of the metrological echoes are weaker than -50 dBm, which is the transition point between the high and low sensitivity channel. The term “online” describes a calibration performed twice during the 5min volume scan by injecting the noise signal in defined range gates where no weather echoes are present.

This publication describes the most important parts of the antenna- mounted receiver (AMR) concept and in particular the inherent radar calibration concept by focusing on the temperature-dependence on the horizontal and vertical receiver chain and the calibration noise source. The receiver temperature dependencies for reasonable day/night cycles derived by field measurement on all Swiss radar sites are verified with lab measurements in a climate chamber. The bias depending on temperature for differential polarimetric measurements (ZDR) is analyzed and discussed. A formula was developed for Selex AMR- radar users to calculate the absolute receiver stability for the elected calibration interval. Finally a recommendation about temporal calibration cycles for AMR systems in European regions is given to assure a continuous accurate absolute radar calibration.

2 Weather radar system design with antenna-mounted receiver

2.1 Antenna Mounted Receiver design

The implemented AMR system design for the Swiss radars is visualized in *Figure 1*. Photographs from the 4.2m dish antenna below the pseudo random cut radome with dual polarization waveguide path and receiver housing unit at the counter weight is shown in *Figure 2*. By looking at such pictures, it is obvious that the receive path is significantly shorter than in conventional system architectures. This leads to a reduction of losses and enhancement of the system sensitivity. In common radar system designs, three waveguide rotary joints are required; one azimuth dual- channel RJ and two elevation single-channel rotary joints. These rotary joints transmission losses are dependent on azimuth- and elevation angle and produce differential phase shifts and amplitude variations for horizontal- and vertical polarization channels. Consequently the

polarimetric products i.e. differential phase (phiDP) and differential reflectivity (ZDR) are affected. The AMR- concept permits the RF high power transmission over one single- channel waveguide rotary joint in azimuth and elevation without the insertion of differential phase- or amplitude biases from rotary joints. The single azimuth rotary joint has a fiber optic rotary joint [2] implemented to allow I/Q data transmission (red signal lines in *Figure 1*) to the signal processor inside the radar control cabinet.

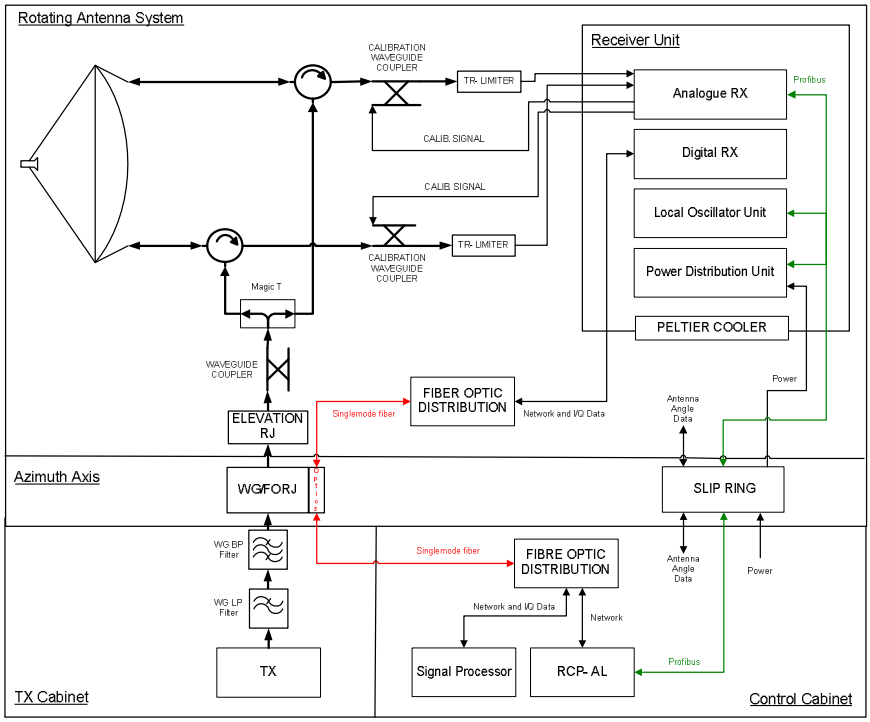

Figure 1: AMR- radar system block diagram [3]

2.2 Receiver unit

The receiver unit houses four 19" racks; power distribution unit, local oscillator unit, digital receiver and analogue receiver also called "Calibration Unit". The calibration unit consists of 4 LNA's to realize the Dynrex [1] solution, two down converter channels for horizontal and vertical polarization and two reference sources for calibration. To calibrate the HI-Sensitive and LOW- Sensitive receiver chains the ITSG-signal will be used for differential phase- and amplitude measurements. The absolute radar calibration will be performed by using the noise source.

Figure 2: Left- dual pol. waveguide path; center- receiver unit; right- AMR. The receiver unit houses the *power distribution unit (5), local oscillator unit (4), digital receiver (3) and analogue receiver also called "Calibration Unit" (2). The Peltier elements are just underneath the receiver unit (9)*

2.2.1 Temperature control for AMR

The temperature within the receiver- housing unit is controlled by active cooling/heating Peltier- elements. On the right picture from Figure 2 the Peltier element unit with its heat sink below the receiver- housing unit is visualized. This module regulates the inner box temperature between the limits for radome temperature ranges of -10°C to 60°C. The internal temperature control is necessary to allocate stable environmental temperatures for the analog and digital receiver components like low noise amplifiers, down converters, oscillators, DSP-boards and the absolute radar calibration device- the noise source.

2.2.2 Thermal noise source verifications in lab

The noise source provides an ENR value of 45dB to overcome the insertion losses of the RF-relays and the 20dB coupling factor of the calibration coupler visible (*Figure 5)*. Finally the noise source generates an absolute dBm value of around -98dBm @ 2.55 MHz bandwidth at the reference point in front of the HI-Sensitive LNA. The pulse width (pw) of 0,5µs occupies for magnetron systems typically 2,4 MHz bandwidth (1.2*1/pw), but recent investigations from [4] have shown, that the bandwidth should be extended with a reasonable factor of 1,064 to calculate the power for noise signals.

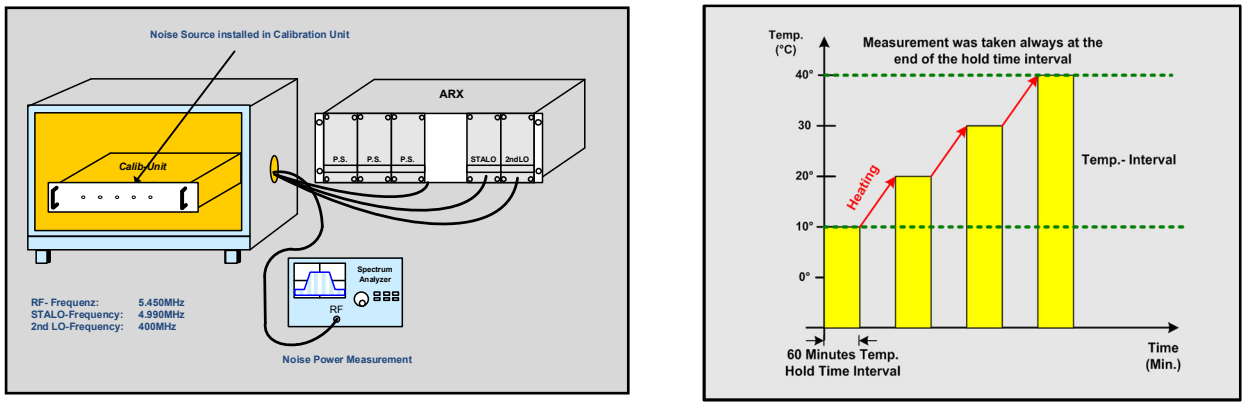

Figure 3: left- Test setup for noise power measurement in an oven; right- Heating procedure

To reach the high ENR value of 45dB the noise source consists of the noise diode unit and the in-line amplifier unit. The rise- and fall times are smaller than 1 µs and from datasheet an excellent temperature dependence of 0.015 dB/K is promised. For implementation in the radar receiver design the ENR values at user frequencies are measured from certified laboratories.

Table 1: Measurement results for noise source power in dBm/Hz

Oven-Temp. °C	Temp. Hold Time Minutes	P_Noise-Out Noise Power (dBm/Hz)
10	60	-129.15
20	60	-129.10
30	60	-128.93
40	60	-128.83

In order to validate the stated temperature- dependency from the noise source datasheet, the noise source within the calibration unit was heated up from 10°C to 40°C (see *Figure* 3- right) in climate chamber and the output power was measured using a spectrum analyzer with suitable noise power measurement software (see *Figure* 3- left). The selected temperature range of 30K and the fact that the noise source is implemented in the calibration unit reflects the operational use of the noise source in the AMR system design. The measurement results in dBm/Hz are stated in Table 1. The noise source output power varies by 0.32 dB/30K, which corresponds to approximately 0.011 dB/K for the temperature interval of interest by assuming linearity. It should be mentioned here that the output power of the noise source is proportional to the temperature. The noise power rises if the temperature increases. This can be explained by using the following equation for calculating the bandwidth- and temperature- depended noise power $N(\mathrm{out})$:

$$N(out) = \mathrm{k} * T_0 * B \qquad (1.0)$$

k represents the Boltzmann constant with 1.38648813*10exp(-23) J/K, T_0 with 283K (10°C) to 313 K (40°C) the current temperature in Kelvin and B the bandwidth, here 1 Hz. By calculating the temperature dependency with equation 1.0, one

would get 0.015 dB/K. The difference between the measured 0.011dB/K and the theoretical calculated value of 0.015 dB/K is probably related to the non-linearity effects of the in- line amplifier to generate the high ENR value of 45 dB.

However, as it will be seen in Sec. 2.2.3, which presents a thorough investigation regarding the receiver-temperature dependence, amplifiers become less efficient if temperature increases. This fact explains the previously mentioned small difference between theory and measurement (0.015-0.011= 0.004 dB/K).

2.2.3 Thermal receiver verifications in lab

To be able to interpret the "online" calibration results generated during the operational scan at the four Swiss radars, a separated receiver- chain measurement took place in the climate chamber. The test setup for measuring the receiver temperature dependencies can be recognized in *Figure* 4 *4*- left with the temperature range of 30K in *Figure* 4 *4*- right, now with 30 min temperature hold time. The continuous wave RF- reference signal was injected by Rhode & Schwarz SMT06 Signal Generator into the receiver reference point and was monitored via Ascope from RAVIS (Radar Visualization Software). The output power was sampled by using the digital receiver (GDRX-RX) at the second intermediate frequency for different temperatures. It should be noted that all receiver components (analog and digital) underlie the temperature drift for creating a comparable situation to the operational AMR.

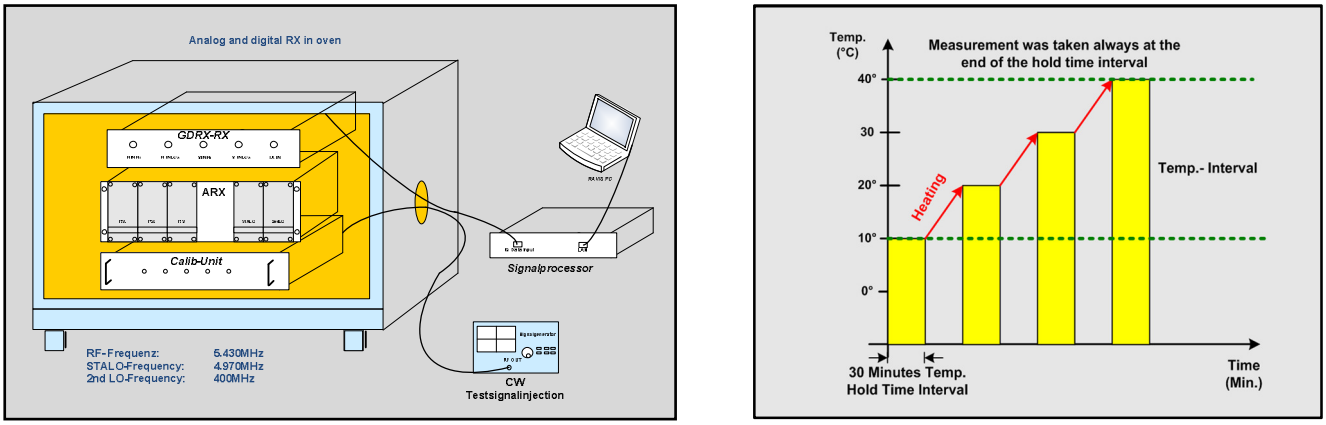

Figure 4: left- Test setup for receiver stability measurement in oven; right- Heating procedure

The results are shown in table 2, which shows the dBadu (logarithmic analog to digital units) values by injecting the CW reference signal into the receiver. A decreasing output signal from 65.23 dBadu -> 63.40dBADU and 65.64 dBadu-> 63.86 dBadu can be recognized. The temperature dependency in H and V channel transfer characteristic can easily be calculated for 1.83 dB/ 30K and 1.78 dB/ 30K for horizontal and vertical received signal, respectively. The receiver channel transfer characteristics show a temperature dependency of 0.061 dB/ K for H-channel and 0.059dB/ K for V- channel. The anti-proportional behavior between increasing temperature and decreasing output signal can be explained by the efficiency drop of the amplifiers within the receiver chains.

Table 2: Measurement results from the digital receiver in dBadu

Oven-Temp. °C	Temp. Hold Time Minutes	Signal Power dBadu_H Horizontal Channel	Signal Power dBadu_V Vertical Channel	Calculated Differential Power dBadu_H -dBadu_V	Calculated Introduced Differential Error
10	30	65.23	65.64	-0.41	-0.04
15	30	64.93	65.36	-0.43	-0.02
20	30	64.65	65.10	-0.45	0.00
25	30	64.38	64.81	-0.43	-0.02
30	30	63.99	64.45	-0.46	+0.01
35	30	63.68	64.17	-0.49	+0.04
40	30	63.40	63.86	-0.46	+0.01

The calculated differential power values from *Table 2* indicate the channel gain differences of the horizontal and vertical receiver chain. The operational radar signal processor considers this difference during the absolute calibration procedure. Meteo Swiss performs the absolute receiver calibration every 5min, so that the temperature dependencies generated by the receiver chains, are calibrated out. Differential changes are also calibrated out by the HI/LOW Calibration procedure. As

long as the repetition cycle of the absolute receiver calibration is short, the radar is well calibrated and is calibration accuracy is only depending on the temperature behavior of the reference noise source signal from table 1. Even if a long calibration cycle (e.g. 12h like day/night cycle) will be selected the induced differential error for ZDR calculations is very small with +- 0.04 dB for temperature range of 30 K. The induced absolute error of 1.83 dB/ 30 K and 1.78 dB/ 30 K by receiver chain is not acceptable without any further calibrations, that's why in 5 a recommendation for AMR absolute calibration cycles will be given, so that the introduced absolute and differential errors from Table 2 can be neglected.

2.2.4 Absolute radar receiver calibration concept with noise source

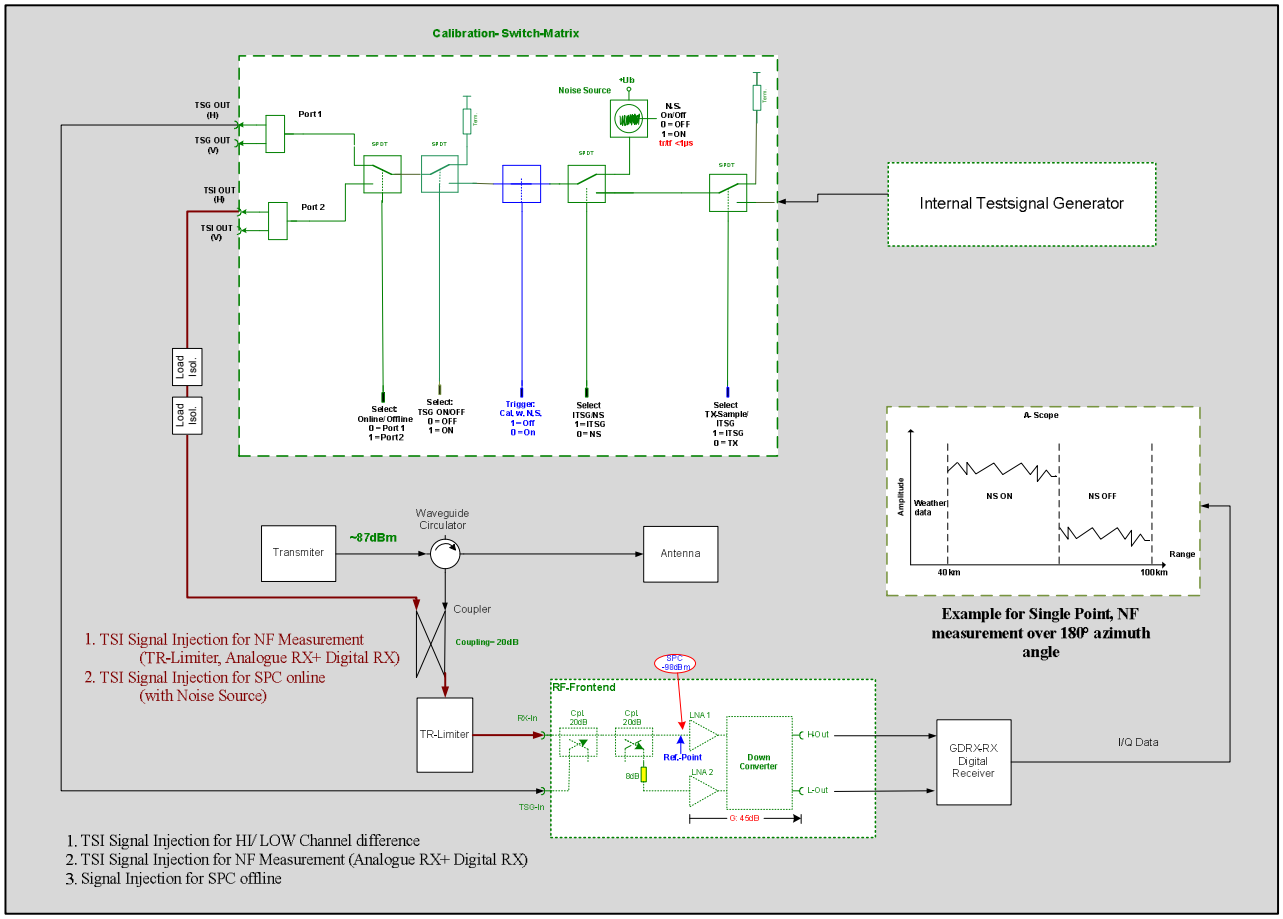

Figure 5: receiver calibration concept

Depending on the position of the RF relays, reference signals from noise source or ITSG can be routed inside the receiver or in front of the TR limiter to perform noise figure measurements, HI/LOW sensitive channel calibrations or absolute radar calibration. MeteoSwiss performs all calibrations every 5 min by injecting the calibration signals during higher elevation scans on ranges where no weather echo are expected.

3 Variance of the fluctuating radar reference signal generated by the Noise Source

A key aspect in the design of the receiver for the Swiss weather radar network is the use of a stable, white, meteorological-like signal as absolute reference (calibration signal), which is continuously monitored every 2.5 minutes. Important positive aspects of this solution are:

- White signal thoroughly and homogeneously filling the whole matched-filter band width;
- High stability and "smaller-than-the-receiver" dependency on temperature;
- The "master", reference signal is used to calibrate the most important channel, which the high sensitivity one;
- The nature of the reference noise signal is by its nature similar to most of hydro- meteorological echoes both in amplitude and in terms of statistical behavior;

Regarding this last topic it is well known that the incoming signal, which is originated by backscattering hydrometeors in the atmosphere and enters into a radar receiver, can be assumed to be Rayleigh distributed. In this Section, we apply the same assumption to the fluctuating radar reference signal generated by the internal Noise Source and we prove that the variance of such signal depends on the number of independent samples averaged. We will also see that the stochastic process can be assumed to be stationary and ergodic of the 2nd order, in the sense that the variance of a realization in time is of the same order of magnitude as the ensemble variance expected from Rayleigh theory.

When interpreting a fluctuating echo, in fact, the usual problem is to estimate its "long-term mean" echo power; in the case of weather targets, for instance, the averaging process aim at obtaining an estimate of the number and size of the scatterers contained in the radar sampling volume (e.g., Doviak and Zrnic (1993) [5]). In the case of atmospheric hydrometeors, since scatterers move with respect to each other as a result of turbulence, shear and varying terminal fall velocities, their radar echo fluctuates from one echo to the next. Thus, the problem arises of estimating the mean echo power from the volume observed, on the basis of a certain number of echoes. This problem has been investigated since the beginning of radar meteorology, see e.g., Marshall and Hitschfeld (1953) [6] and Wallace (1953) [7], among others. When estimating the "long-term mean" power from the inherently fluctuating Rayleigh signals, one could average either the echo power intensities or the echo logarithmic levels. As shown in Fig. 2 in the paper by Zrnic (1975) [8], averaging the echo intensities provides smaller variance values, for the same number of independent samples. The short note by Gabella (2014) [9] presents analytical expressions of the variance of the two typical estimators of mean values of echo power: the 1st one is based on echo intensities; the 2nd one is based on echo logarithmic levels (see also Fig. 1 in [9]). Consequently, it is better to average echo intensities rather than logarithms. With the availability of digital IF receivers, which facilitate the averaging of echo power, the result has a practical value.

The analytical formulas presented in [9] are also useful to estimate the variance of radar receiver thermal noise as well as the calibration reference signal generated by the Noise Source, once that the number of averaged samples is known. Prior to the envelop detector (rectification), which means energy detection in the electronic circuit, receiver noise (both thermal and Noise Source generated) is expected to have a Gaussian distribution with a zero mean. After rectification, such noise has an exponential one-sided probability distribution that fluctuates around a mean, which is the root-mean-squared value of the unrectified fluctuations. In other words, the results by Marshall and Hitschfeld (1953) [6], which were related to the treatise on sound by Lord Rayleigh (1877) [10], also apply to noise signals (thermal or generated by the Noise Source) entering the receiver. Actually, the assumption of Rayleigh fluctuations for thermal noise is probably even less controversial than for precipitation scatterers: the assumption of "all nearly equal scatterers" (i.e., no few scatterers dominate) for hydrometeors, in fact, requires "near statistical stationarity" or, equivalently, "near statistical homogeneity" of the hydrometeors in space.

Furthermore, in the case of noise, it is possible to assume that the number of available samples, *M*, coincides with the equivalent number of independent samples, *N*, which, throughout this Section, has been used to express the reduction in estimate variance that can be achieved by averaging. On the contrary, in the case of hydro-meteorological echoes, a considerable correlation may exist from one echo to the next one, given the typical pulse repetition frequency of meteorological radar. For example, Doviak and Zrnic (1993, Section 6.3.1.2) [1], presented the variance reduction factor for the square-law receiver as a function of the raindrop Doppler velocity spectrum width, the unambiguous velocity, and the total number of weighted samples, M.

In the next sub-Section, we present a practical example and applications of the derived analytical formulas listed in [9] and related to the variance of the fluctuating radar signal from noise and randomly distributed scatterers; the Section deals with real noise source data measured by the horizontal and vertical receiver chains with a demonstrator in Selex laboratories (Neuss, Germany) during Calendar Week 17 (2014).

3.1 The experiment at the Selex facilities

The first experiment started on April 23 at 14:56:30 UTC; the former Monte Lema calibration unit (L.1) was used to inject every 2 seconds the reference signal into the receiver (GDRX) of a demonstrator radar at Selex facilities. The experiment ended on April 24 at 08:51:31 UTC. The number of available values is 32146 for both the Horizontal and Vertical channel. Each value delivered by the GDRX is in turn the average of 3000 pulses sampled at the same 83.3 m gate. Main statistical parameters (central location and dispersion) of this huge (32146 elements) temporal realization are shown in Table 3.

Let us start from the analysis of the whole realization (lines 3 and 4): for both channels, probability density functions are symmetric; the median is close to the mean; the spread, which is (84%tile-16%tile)/2, is even coincident (3 decimal figures) with the standard deviation. Then we have simply split the data set into 2 parts with the same number of elements (16073). It is evident that such random process can be assumed to be stationary of the 2nd order: the standard deviation of the two subsets is practically coincident for both channels; also the average value of the two subsets is quite close (both H and V); again, all distributions are quite symmetric, with standard deviation very close to the spread. Xxx By way of example, the 2 pictures below shows the probability density functions of the vertical channel for subset 1 and 2 (lines 5 and 6 in Table 3).

Table 3: Statistical characterization of the Noise Source signal in terms of central location and dispersion

Channel	Data set	Number of Samples	Average dBm	Median dBm	spread dB	Standard Deviation dB
Horizontal	Subset 1	16073	-92.348	-92.350	0.080	0.081
Horizontal	Subset 2	16073	-92.344	-92.340	0.085	0.081
Horizontal	whole	32146	-92.346	-92.350	0.080	0.081
Vertical	whole	32146	-92.431	-92.430	0.080	0.081
Vertical	Subset 2	16073	-92.437	-92.440	0.080	0.082
Vertical	Subset 1	16073	-92.425	-92.420	0.080	0.081

An interesting exercise is certainly to test whether the random (Noise Source) process can also be assumed ergodic. If noise, just like randomly distributed scatterers (e.g. hydrometeors in the atmosphere), were Rayleigh distributed, then we could use Eq. (10) of [9] for assessing the expected standard deviation of such experiment. Since for noise it is even possible to assume a Dirac delta as the autocorrelation function (in practice, each pulse, PRT=0.6666 ms, PRF = 1500 Hz, is for sure statistically independent from the next one), then the number of independent samples N can be assumed to be equal to 3000. As a consequence, Eq. (10) becomes

$$\sigma = 10\cdot(\mathrm{Log}e)\cdot\sqrt{\frac{\pi^2}{6}-\sum_{k=1}^{2999}\frac{1}{k^2}} = 10\cdot(\mathrm{Log}e)\cdot\sqrt{\frac{\pi^2}{6}-1.6446} = 0.0664\ \mathrm{dB} \qquad (2.0)$$

Adding up, from theoretical speculations we would expect an ensemble standard deviation of 0.066 dB; in practice, from a single realization (or two subsets from the same temporal realization) we get a standard deviation which is slightly worse, namely 0.081 dB; anyhow, the time-based estimate of the standard deviation is not too different from the ensemble estimate: hence, we conclude that the random process generated by the noise source and measured by the GDRX can be assumed to be quasi stationary and ergodic with respect to the dispersion.

The noise source is able to provide a stable reference signal; its uncertainty depends on the number of pulses averaged by the radar signal processor: with one single pulse it tends to the intrinsic value of 5.57 dB. For N>1, the exact solution when averaging echo power values is presented in Eq. (10) of [9]. When N is very large, the advantage of a smaller variance associated to an arithmetic average of power values (with respect to averaging directly logarithmic levels, i.e. geometric average) becomes less and less pronounced. In our example, the ensemble standard deviation of a geometric average turns out to be $5.57/3000^{0.5}$ = 0.102 dB instead of 0.066 dB, as shown by Eq. (9) in [9].

4 Receiver temperature dependency

As described in Chapter 2.2.4, the online calibration of the receiver chain is performed every 5' during the operational Swiss scan. The measured values are then saved as analog-to-digital units (adu) in a status files, which also contains over 200 additional status parameters, sampled once for every sweep (20 sweeps per volume, e.g. 20 values for each parameter). Among these parameters there are over 10 different temperature values, recorded from sensors placed in critical position of the system. Two of these sensors are placed within the receiver unit, which is housing the calibration unit, and monitor its environment temperature; the measured temperatures values of one of these sensors are used to show the dependence of the measured noise source signal with temperature during the online calibration, under different temperature conditions.

The following radar systems and time intervals have been chosen for the analysis:

- Radar Albis (Canton of Zurich, 935m asl); 13.05.14 – 17.05.14
- Radar Monte Lema (Canton of Ticino, 1627m asl); 08.07.14 – 12.07.14
- Radar Plaine Morte (Canton of Valais, 2937m asl); 29.12.13 – 30.12.13

4.1 Radar Albis 13.05.14 – 17.05.14

In *Figure* 6 the noise source power (plotted as logarithmic adu values dBadu) and the receiver unit temperature (°C) are plotted as a function of time, for a period of 5 days. The data are plotted every 5 minutes.

A day-night cycle can be clearly recognized when following the temperature fluctuations from left to right, low value in the early morning and high values in the mid-afternoon. This pattern is evident from 13.05 (00:00) to 16.05 (12:00). For this time interval, an inverse correlation with the measured noise source power can be observed: high noise source values (between 32.75 dBadu and 32.80 dbadu) are measured in correspondence with the lowest measured temperatures (early

morning, between 23.5°C and 24.0°C). When a specific threshold temperature inside the receiver box is reached, in this case between 26.0°C and 26.5°C, the Peltier elements within the receiver box is activated and an environmental cooling intervenes. This is the reason for the scatter in the temperature values starting from Mai 16, 12:00. The overall temperature in the receiver box is of course dependent on the overall temperature in the radome. A temperature > 17°C in the radome, which corresponds to a temperature of ca. 26°C in the receiver unit, will trigger the Peltier elements within the receiver unit. In these intervals, the measured noise source power show values between 32.55 dBadu and 32.6 0dBadu.

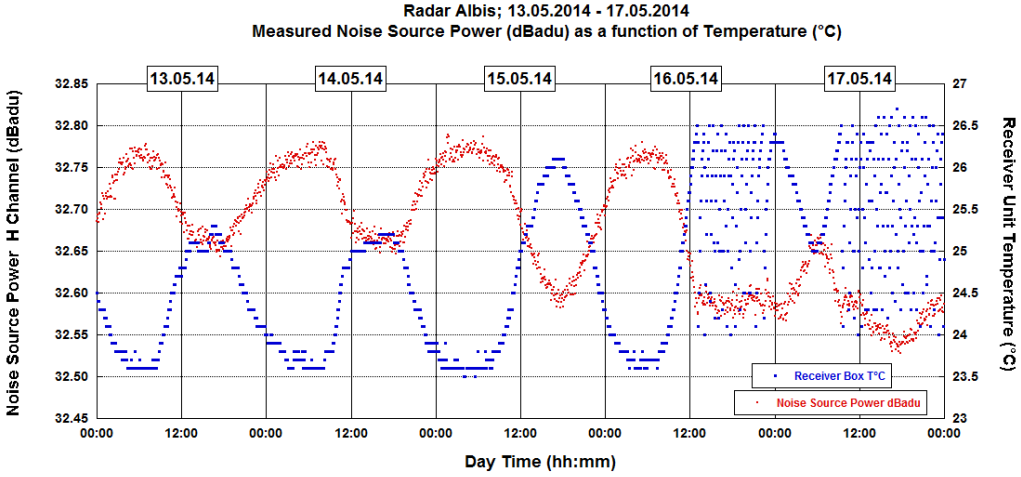

Figure 6:
Noise source power (in analog-to digital logarithmic units dBadu) and temperature of the receiver Unit (°C) are plotted as a function of time for the radar Albis, from Mai 13 to Mai 17, 2014. The measurements are plotted with a resolution in time of 5'. A clear inverse correlation between noise source power and temperature can be observed from Mai 13 to Mai 1 at 12:00. The scattered temperature values on Mai 16 and Mai 17 are caused by the Peltier elements in the receiver unit, keeping temperature below ca. 26.5°C.

4.2 Radar Monte Lema 08.07.14 – 12.07.14

In *Figure* 7 the noise source power and the receiver unit temperature are plotted as a function of time, for a period of 5 days. The noise source power data are sampled every 5', the temperature values are plotted with 20 values every 5' (1 value for each sweep of the volume scan).

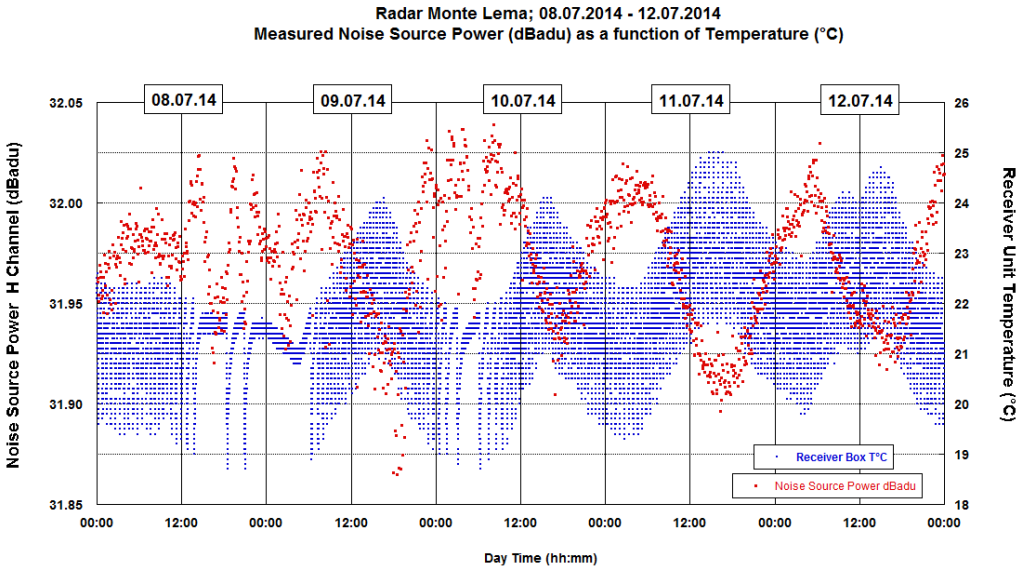

Figure 7:
Noise source power (in analog-to digital logarithmic units dBadu) and temperature of the receiver Unit (°C) are plotted as a function of time for the radar Monte Lema, from July 8 to July 12, 2014. The noise source measurements are plotted with a resolution in time of 5'; 20 temperature values are available every 5' (one value for each sweep of the volume scan). For the majority of the time, the Peltier elements was active, trying to lower the environment temperature of the receiver box. An inverse correlation between noise source power and temperature can be observed; this pattern was also observed in Figure 6.

The first observation is that for the analyzed interval, the Peltier elements is almost always active. This is indicated by the temperature band, 2°C to 3°C wide across the plot. We can nonetheless recognize day-night cycles, which are reflected by the measured noise source values, showing an anti-correlation pattern as in *Figure* 6.

In *Figure* 8 a detail of *Figure* 7 is shown, namely the behavior of the measured noise source power and temperature for July 11. The temperature cycles of the Peltier elements are easily recognizable, as well as the overall day-night cycle which is affecting the radome temperature. The superimposed noise source power data show the typical behavior (anti-correlation) described in *Figure* 6.

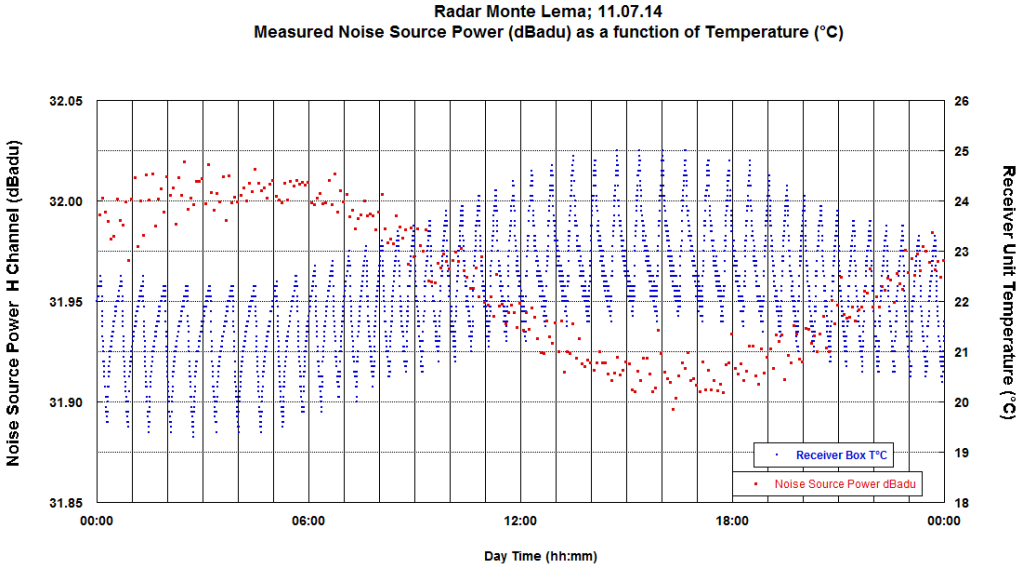

Figure 8:
Noise source power (in analog-to digital logarithmic units dBadu) and temperature of the receiver Unit (°C) are plotted as a function of time for the radar Monte Lema, for July 11, 2014 (detail from Figure 7). The noise source measurements are plotted with a resolution in time of 5'; 20 temperature values are available every 5' (one value for each sweep of the volume scan). The cooling cycles of the Peltier elements can be recognized, as well as the noise source measurements pattern, inversely correlated with the overall temperature trend.

In *Figure* 7, two time intervals during which the Peltier elements was mainly not active (July 8 afternoon – July 9 morning and July 10 morning) can be recognized, one of these is shown in detail in *Figure* 9. Four different cooling cycles can be observed. Minima on the measured noise source power can be observed when temperature stability is obtained over a relatively long period after the cooling cycles has ended. The highest measured noise source values (above 32 dBadu) are observed just after the following heating up occurs (ca. 30'-40' later).

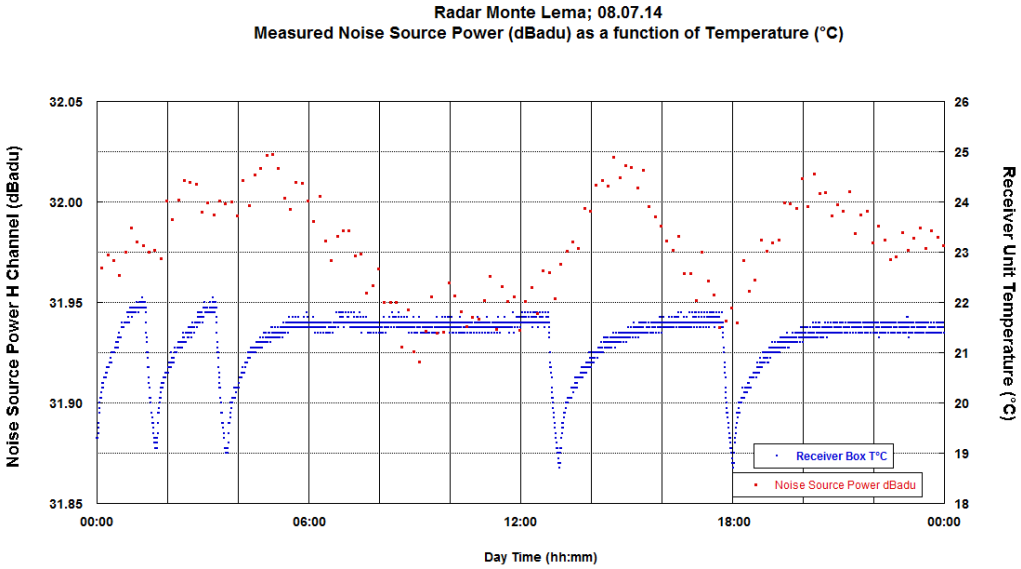

Figure 9:
Noise source power (in analog-to digital logarithmic units dBadu) and temperature of the receiver Unit (°C) are plotted as a function of time for the radar Monte Lema, for July 8, 2014 (detail from Figure 7). The noise source measurements are plotted with a resolution in time of 5'; 20 temperature values are available every 5' (one value for each sweep of the volume scan).

4.3 Radar Plaine Morte 29.12.13 – 30.12.13

A couple of month after having installed the new radar system at Plaine Morte, we had a failure on the heating system of the radome. We were daily monitoring the temperature trend from remote, and eventually restored the heating system.

The radar system was working during this period, the temperature within the receiver unit reached a minimum of ca. 9°C and increased to ca. 22°C, as soon as the heaters were re-activated. Under these conditions it was possible to monitor the behavior of the noise source over a wide range of temperatures. In *Figure 10* this event is represented for a time interval of two days (December 29 and 30, 2013).

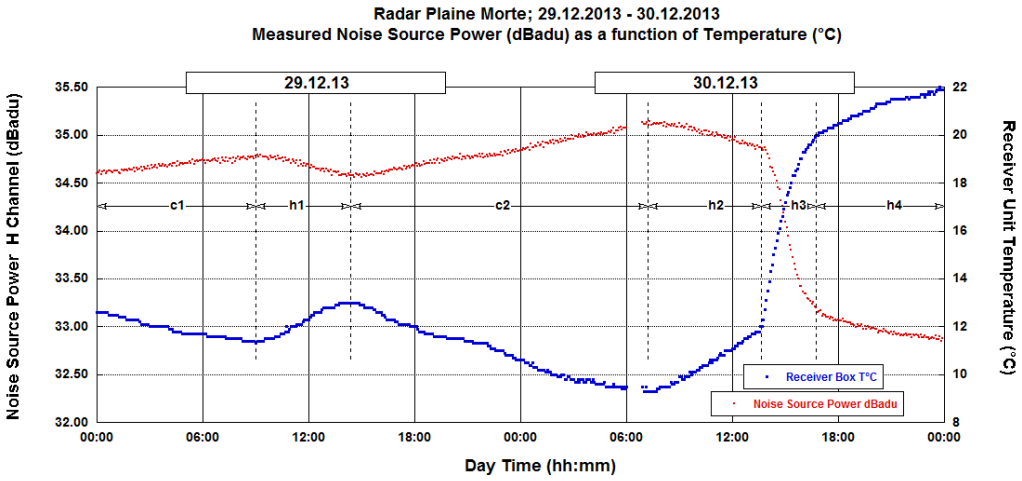

Figure 10:
Noise source power (in analog-to digital logarithmic units dBadu) and temperature of the receiver Unit (°C) are plotted as a function of time for the radar Plaine Morte, from December 29 to December 30, 2013. The measurements are plotted with a resolution in time of 5'. Note the high temperature range in this example, from ca. 9°C up to 22°C, causing a variation of the measured noise power of ca. 2 dB. The plotted interval has been divided in different cooling (c1 and c2) and heating (h1 to 4) time intervals, which have been analyzed separately, in order to retrieve a power-temperature correlation function (see text below.)

As in the previous *Figure* 6 and *Figure* 7, the expected inverse correlation between measured noise power and temperature can be observed. For this data we tried a more quantitative approach, and tried to establish the relationship between noise source power and temperature, this for six different time intervals, two cooling intervals (c1 and c2) and four different heating intervals (h1 to 4). A linear regression between noise source power P (dBadu) and temperature T(°C) was derived. The results of the fit (offset, slope and explained variance, which is square of the correlation coefficient in percentage) for the given time intervals are as follow:

- C1: P(T) = 36.2 – 0.13·T; r^2= 91.6% (110 samples)
- C2: P(T) = 36.4 – 0.14·T; r^2= 96.9% (238 samples)
- H1: P(T) = 36.1 – 0.11·T; r^2= 93.6% (65 samples)
- H2: P(T) = 36.1 – 0.10·T; r^2= 95.2% (78 samples)
- H3: P(T) = 38.0 – 0.23·T; r^2= 93.1% (25 samples)
- H4: P(T) = 36.8 – 0.13·T; r^2= 95.3% (89 samples)

As a term of comparison, the same relationship can be calculated for the data from the radar Albis (from 13.05 (00:00) to 16.05 (12:00):

- P(T) = 34.7 – 0.07·T; r^2= 94.9% (1437 samples)

4.4 The influence of temperature on the Horizontal and Vertical receiver channels

In *Figure* 6 to 10, the analysis was performed by studying the relationship between one receiver channel (Horizontal channel H) and temperature. In order to establish the temperature dependence of both channels, the difference H(dBadu)-V(dBadu) was analyzed for the above events. An absolute comparison between channels and between radars should be performed by comparing absolute power values (in dBm) and not digital power values (dBadu). This is the reason why we limit our analysis to dispersion of such differences: Standard deviation values are listed for the three above mentioned examples:

- Albis St.Dev: 0.0162 dBadu
- Monte Lema St.Dev: 0.0073 dBadu
- Plaine Morte St.Dev: 0.0064 dBadu

4.5 Temperature reliability measurements

This analysis has been performed using one particular temperature sensor, whose task is actually that of monitoring the overall temperature in the receiver unit, and not of a given specific component. There are up to five temperature sensors in the receiver unit; the measured temperature depend on their physical placement within the receiver unit. In this sense, it is difficult to infer the exact temperature of the noise source during operation. Nevertheless, the relative temperature excursions measured by the different sensors are almost the same. This means that the overall temperature equilibrium can be assumed to be reached relatively fast in the receiver unit, which is an indication of a generally good air circulation within the receiver unit. An intermittent cooling forced by the Peltier, as shown in *Figure* 9, can nonetheless introduce a time lag between the measured temperature by the five sensors and the actual temperature of a single component, in our case the noise source.

5 Calibration interval recommendation for AMR systems

In the Swiss Rad4Alp radars the stability of the Selex receiver integrated in a AMR design was thoroughly investigated. The investigation revealed a temperature drift of the complete receiver without calibration of ca. -0.07 dB/K to -0.23 dB/K, this under normal (as for Albis, with small variation in temperature) and extreme (as for Plaine Morte, with up to 13°C variation) operational conditions. Furthermore, the temperature drift in H and V channel is well correlated and has no major impact on ZDR, since both receiver channels share the same housing. With calibration, the temperature stability of the noise source was almost completely transferred to the receiver.

Equation 3.0 gives operational AMR radar system users the expected absolute receiver accuracy for the selected calibration cycle at the prevailed on Site temperature drift for the day/night cycles. For mid-latitude regions a calibration cycle of 1 calibration every 1-2 hours for the AMR- design can be recommended. For stronger absolute calibration requirements or higher environmental temperature gradients (or no air- conditioning in radome) the calibration cycle should be scaled down.

$$RX\,{}^{Accuracy}_{Cal.Cycle} = \pm\frac{T_{Day/Night} * N * RX_T}{24h * 2} \qquad (3.0)$$

Calculation- example for the radar Site Albis:

$T_{Day/Night} = 2.5\,K$; $RX_T = 0.07 dB/K$; $N = 12\,h$

$$RX\,{}^{Accuracy}_{Cal.Cycle} = \frac{2.5\text{K}}{2 * 24\text{h}} * 12\text{h} * 0.07\frac{\text{dB}}{\text{K}} = \pm 0.044\ \text{dB}$$

The result of ± 0.044 dB from the Albis calculation example describes the established radar receiver accuracy for a user selected calibration cycle of $N = 12\,h$. The temperature gradient of the day/night cycle with $T_{Day/Night} = 2.5\,K$ was used from Figure 6 (13.05.14 to 14.05.14).

Calculation- example for the radar Site Plaine Morte:

$T_{Day/Night} = 13\,K$; $RX_T = 0.23\,dB/K$; $N = 1\,h$

$$RX\,{}^{Accuracy}_{Cal.Cycle} = \frac{13\text{ K}}{2 * 24\text{h}} * 1\text{h} * 0.23\frac{\text{dB}}{\text{K}} = \pm 0.062\ \text{dB}$$

The result of ± 0.062 dB from the Plain Morte calculation example describes the established radar receiver accuracy for a user selected calibration cycle of $N = 1h$. The temperature gradient of the day/night cycle with $T_{Day/Night} = 13\,K$ was used from Figure 10 (29.12.13 to 30.12.13). It should be noted/repeated here, that the strong temperature gradient of 13K was produced by a malfunction of the radome- heater on radar site.

Acknowledgement

For continuous radar operation and the development of such complex radar systems many people are involved. We would like to thank the whole development, commissioning and production department from Selex-ES for the assistance in system design and project management board for the good team work during the hot research and development phase in 2009. We would also like to thank the MeteoSwiss Rad4Alp project.

References

[1] **Gekat, F. and Rühl;** Multi-Channel Radio Frequency Receiver, Patent Number: EP 1908174, D., 2005.

[2] **Vollbracht, D.; Gekat, F.; Hilger D.; Hille M.;** "Waveguide Fibre Optic Rotary Joint for Antenna Mounted Radar Receivers", 34th International Conference on Radar Meteorology, AMS Conference, October 2009.

[3] **Vollbracht, D.; Ridene, D; Gekat, F.;** "Receiver over Elevation (ROEL) Weather Radar System Design and its Advantages", 12th URSI Commission F Triennial Open Symposium on Wave Propagation and Remote Sensing, Garmisch-Partenkirchen, March 2011

[4] **Gölz, P.; Vollbracht, D.; Gekat, F.;** "Calibration of a weather radar receiver with a noise diode", 36th Conference on Radar Meteorology, AMS Conference, September 2013.

[5] **Doviak, R.J., Zrnic, D.S**.; *Doppler Radar and Weather Observations*, 2nd ed.; Academic Press: Waltham, MA, 1993.

[6] **Marshall, J.S., Hitschfeld, W.;** Interpretation of the fluctuating echoes from randomly distributed scatterers, Part I. *Can. J. Phys. 31*, 962–994, 1953.

[7] **Wallace, P.R.**; Interpretation of the fluctuating echoes from randomly distributed scatterers, Part II. *Can. J. Phys. 31*, 995–1009, 1953.

[8] **Zrnic, D.S.**; Moments of estimated input power for finite sample averages of radar receiver outputs. *IEEE Trans. Aerosp. Electron. Syst*. *11*, 109–113, 1975.

[9] **Gabella M.**; Variance of Fluctuating Radar Echoes from Thermal Noise and Randomly Distributed Scatterers, Atmosphere, 5, 92-100, 2014.

[10] **Rayleigh, J.W.S., Lord.**; *The Theory of Sound*; Macmillan: London, UK, 1877; Volume I, Reprinted version, in 1945 by Dover Publications, p. 984